ISSN 1392–1320 MATERIALS SCIENCE (MEDŽIAGOTYRA). Vol. 28, No. 4. 2022

Study on the Microstructure and Wear Behavior of In-Situ Al_3Ti/Al Composites Under Induction Heating

Yuting YAN [1], Libin NIU [2]*, Anwen ZHANG [1], Chengxin LIU [1], Zhidong FAN [1], Yichao MA [1]

[1] *Xi'an Thermal Power Research Institute Co., Ltd., Xi'an 710054 China*
[2] *College of Materials Science and Engineering, Xi´an University of Science and Technology, Xi'an 710600, China*

crossref http://dx.doi.org/10.5755/j02.ms.28724

Received 26 March 2021; accepted 10 June 2021

In the study, Ti fiber (200 μm, 99.8 wt.%) and pure aluminum (99.6 wt.%) were respectively used as the reaction source and matrix to prepare Al-based composites by in-situ synthesis methods. During the stage of preparing the preform, Ti fibers were fixed in the matrix at equal intervals to pre-control the initial position of the product. The preform was heated in an induction heating device finally, at the same time, parameter combinations of different frequencies and currents were applied to promote the in-situ reaction between Al-Ti, thereby the Al matrix composites reinforced by Al_3Ti were obtained. The phase composition, microstructure and wear resistance of the composites were characterized by X-ray diffraction (XRD), scanning electron microscopy (SEM) and wear testers. The results show that when the frequency and current are 5 kHz and 15 A respectively, the Ti fiber is completely reacted, and the product is the isometric Al_3Ti with a size of 1 – 2 μm and a particle spacing of about 5 μm, reaching the optimal microstructure under all parameters. Under the condition of a load of 9.8 N, the wear rate of the composites at 5 kHz and 15 A is 2.325 mg/mm^2, indicating the best values in this experiment.
Keywords: titanium fiber, In-situ reaction, frequency, wear behavior.

1. INTRODUCTION

Due to the properties of high hardness and high wear resistance, ceramic particles such as SiC and TiB_2 as a reinforcing phase have been widely used in wear-resistant parts of aluminum-based composites [1]. However, the physical properties of the aluminum matrix and the ceramic particles are quite different, such as the coefficient of thermal expansion, which leads to greater stress when the two materials are combined, and the reinforcement phase is easily peeled off during service, affecting the wear resistance. Compared with ceramic particles, the Al-Ti intermetallic compound is used as the reinforcing phase of the aluminum matrix to eliminate the stress due to similar physical properties [2], and the wear resistance is improved obviously. Among them, in-situ formed Al_3Ti particles have attracted increasing attention because of low density (3.4 g/cm^3), high hardness and strong wear resistance [3].

The in-situ endogenous particle method, as the most important method for preparing particle-reinforced metal matrix composites, the reinforcement phase is generated through internal chemical reactions, which avoid defects such as surface pollution, poor wettability of the reinforcement and the matrix. Recently, the in-situ reaction between Al melt and Ti powers was studied by Liu [4]. It was reported that the shape of Al_3Ti was blocky with a size of 7 μm and exhibits excellent wear resistance. Qin [5] prepared in-situ Al_3Ti particles by ultrasonic vibration, and the reaction-peeling model was established to explain the formation mechanism of blocky Al_3Ti. Gupta [6] prepared in-situ Al_3Ti particles under high stress and high temperature and improved the composites dispersibility through ultrasonic vibration. However, the distribution of the Al_3Ti particles prepared by this method is uncontrollable and cannot be concentrated in a designated area, leading to low utilization of raw materials. Besides, the lack of external power increases the reaction rate during the in-situ endogenous process, resulting in prolonged reaction time, and the reinforcing phase is easy to grow and agglomerate [7].

Aiming at the above shortcomings, such as poor uniformity of Al_3Ti and slow in-situ reaction rate, the author designed a new process for preparing Al-based composites as a solution. At the stage of preparing the preform, Ti fibers are fixed to the mold at equal intervals, ensuring that the initial uniformity of the Ti source before the reaction starts. At the stage of heating the preform, the in-situ reaction is provided with additional power which is produced by the induction heating furnace, and the reaction rate is increased.

During the induction heating process, the sample is heated by the induced current generated by the alternation current. The size, shape, and dispersion of Al_3Ti particles are dominated by the alternation current parameters and affect the properties of the composites. In this paper, the optimal parameters of the frequency and current of the alternation current are confirmed, and the influence mechanism is studied, which provides the basis for the process of preparing Al_3Ti/Al composites.

*Corresponding author. Tel.: 029-85587373.
E-mail address: *nlb13319213034@xust.edu.cn* (L.B. Niu)

2. EXPERIMENTAL PROCEDURES

2.1. Synthesis of Al_3Ti/Al composites

In this experiment, Ti fiber (99.8 wt.%) with a diameter of 200 μm was used as the reaction source, and pure aluminum (99.6 wt.%) was used as the matrix. The molten pure aluminum was poured into the preheated mold (200 ℃), which was lined with graphite paper to prevent the aluminum liquid from being oxidized. And the mold was fixed multiple Ti fibers at equal distances in advance to ensures that multiple sets of data under the same batch of parameters are obtained, as shown in Fig. 1 a. When the sample was cooled, it was cut into the R8 mm × 20 mm preform shown in Fig. 1 b. Finally, the preform was placed in an induction heating furnace (Fig. 1 c) for induction heating under different parameter combinations, to prepare the Al_3Ti/A composites.

The frequency of the induction heating furnace was set to three levels, namely low frequency (50 – 100 Hz), intermediate frequency (1 – 9 kHz), high frequency (10 kHz and above), and the current was set in equal gradients under 0 – 20 A. By referring to the previous research progress of this research group [8], the induction heating process was carried out according to the parameters in Table 1, and the infrared thermometer was fixed for real-time temperature measurement during the whole process.

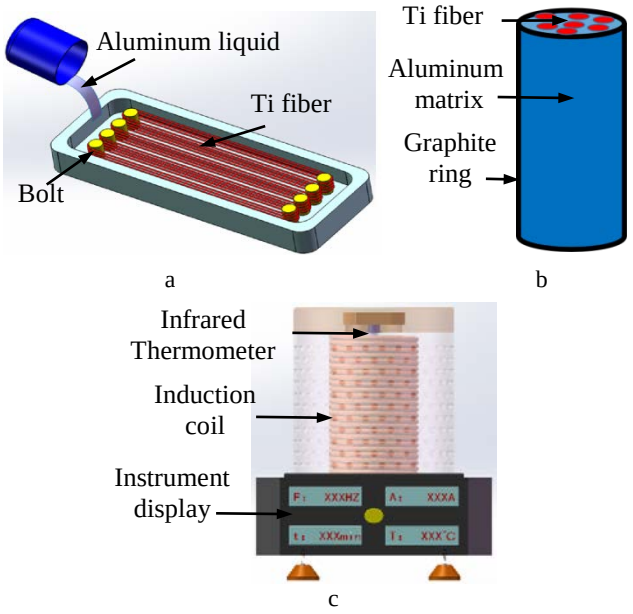

Fig. 1. Schematic diagram of the composites preparation process: a – casting equipment; b – composite preform; c – induction heating device

Table 1. Numerical table of parameter combination

No.	A	B	C	D	E
Frequency, Hz	100	1k	5k	5k	10k
Alternating current, A	5	10	15	20	15
Time, min	10				

2.2. Characterization of Al_3Ti/Al composites

To investigate the effects of parameter combinations on the phase constituents of the composites, phase constituents were studied by PW1730 X-ray diffraction (XRD) with monochromatic Cu-Kα radiation (40 KV, 40 mÅ). The microstructure and phase constituents of the composites were investigated using a field emission scanning electron microscope (VegaIILMU) with an energy dispersive spectrometer (EDS).

2.3. Wear resistances test

The wear resistance of the processed surfaces was studied by a two-body abrasive wear tester (ML-100) with a reciprocating configuration. The specimen (diameter 6 mm and length 30 mm) was loaded against a rotating disk (25 rpm) covered with a 240 mesh SiC abrasive paper under the load of 9.8 N. To ensure fresh supply of abrasive particles to the specimen, the worn SiC abrasive paper was replaced with the new one for every sliding distance of 10 m. The wear resistance test was repeated at least three times, and each test lasts for one minute. The wear rate of the specimen is evaluated by the weight loss per unit area, and the weight loss of the specimen was measured in an electronic balance with an accuracy of 0.0001 g. After the two-body abrasive wear test, SEM was used to analyze the surface wear marks.

3. TEST RESULTS

3.1. Phase composition of Al_3Ti/Al composites

XRD patterns of the composites under different parameters are shown in Fig. 2.

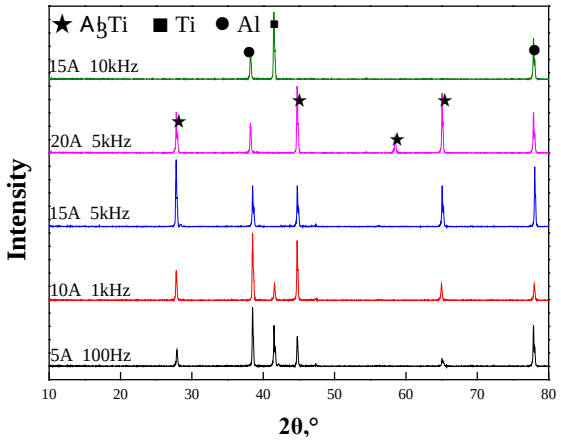

Fig. 2. XRD patterns of Al_3Ti/Al at different parameter combination

The composites obtained by 100 Hz and 5 A were composed of Al, Ti and Al_3Ti. The existence of the Al_3Ti diffraction peak proved that the in-situ reaction between the Ti fiber and the Al matrix had occurred. The Ti diffraction peak existed, however, indicating that the degree of reaction between Al-Ti was weak. As the frequency and current were increased to 5 kHz and 15 A respectively, the composites were composed of Al and Al_3Ti diffraction peaks, and the absence of Ti diffraction peak indicated that the Ti fiber had been reacted completely.

The composites were composed of Al matrix and Al_3Ti when the frequency was fixed to 5 kHz and the current was increased to 20 A. However, a new Al_3Ti

diffraction peak appeared at 58°, which indicated that Al_3Ti with the $D0_{23}$ crystal structure appeared in the phase composition [9]. A previous study reported that the Al_3Ti with a crystal structure of $D0_{23}$ could be obtained from the transformation of $D0_{22}$ and the unstable state of $L1_2$[10], proving that the crystal structure of Al_3Ti was transformed under this parameter.

When the current was fixed at 15 A and the frequency was increased to 10 kHz, there were Ti and Al diffraction peaks in the phase curve of the composites, and no other products were found, proving that the Al-Ti reaction did not occur.

3.2. Microstructure of Al_3Ti/Al composites

The microstructure of the composites prepared at 100 Hz and 5 A is shown in Fig. 3. The bright white structure was Ti fiber with a diameter of 120 μm. The Ti fiber was surrounded by the gray product layers, and the gray particles moved outward gradually, as shown in Fig. 3 a. A magnified observation of the Ti fiber boundary in Fig. 3 b revealed that the particles were peeled off along the crushing channel. However, the moving distance of the particles was relatively short, still surrounding the Ti fiber. The magnified figure showed that the gray particles were surrounded by black shadows. There were protrusions between the particles and the matrix, leading to a decrease in binding force.

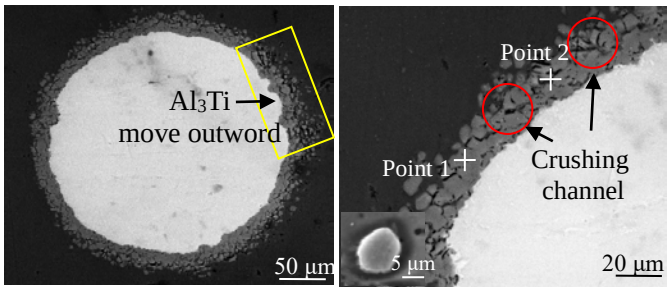

a b

Fig. 3. Al_3Ti/Al composites under 100 Hz and 5 A: a – low magnification; b – crushing channel and particle morphology

The point EDS analysis of the gray particles was carried out to obtain the atomic ratios of elements at different positions, as shown in Table 2. The gray particles produced by the Al-Ti reaction were Al_3Ti, which was analyzed by the atomic ratio of Al/Ti at point 1 and point 2 was 3:1.

Table 2. Phase EDS analysis of different point position

No.	Point 1	Point 2	Point 3	Point 4
Al, at.%	74.26	76.19	75.16	76.25
Ti, at.%	25.74	23.81	24.84	23.75
Total	100	100	100	100

In this experiment, pure aluminum was heated in an induction heating furnace simultaneously, and the time-temperature curve was drawn. By comparing the real-time temperature of pure aluminum and composites, the in-situ reaction temperature of Al-Ti was directly measured, and the temperature curves were shown in Fig. 4. When the current was 5 A and the frequency was 100 Hz, the temperature of pure aluminum and composites increased synchronously within 0 – 8 min. The temperature curves were separated at 8min30s because of the heat released from the reaction of Al-Ti. The separation temperature was 627.5 ℃, which was the reaction temperature. This temperature was significantly lower than the Al-Ti reaction temperature (890℃) explored by this research group when the resistance furnace was used for heating [11].

As the frequency and current were increased to 1 kHz and 10 A respectively, the area of the reacted Ti fiber increased. The coverage area of the product increased and the drift distance of the particles became longer in Fig. 5 a, which indicated that the dispersion performance of the composites was enhanced. EDS analysis of point 3 and point 4 revealed that the atomic ratio of Al/Ti were both 3:1, and it was judged that the particles peeled off from the product layer were Al_3Ti, and there is no other Al-Ti intermetallic compounds were generated. As the Al_3Ti particles were magnified, it was found that no black shadows were formed on the edges, indicating that the bonding force between the Al matrix and Al_3Ti was enhanced due to the flatness.

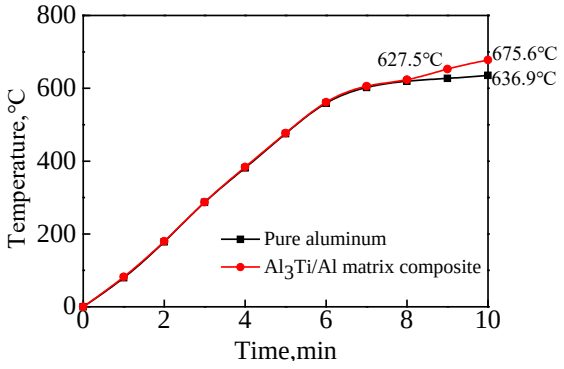

Fig. 4. Real-time temperature curve of pure aluminum and composites at 100 Hz and 5 A

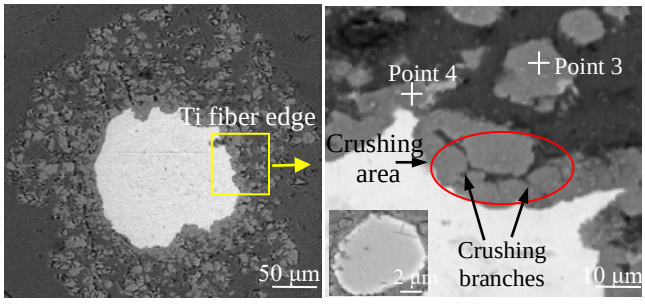

a b

Fig. 5. Al_3Ti/Al composites under 1 kHz and 10 A: a – low magnification; b – crushing area and crushing branches

There were more channel branches extending to the Ti fiber, as shown in the red area of Fig. 5 b. It was indicated that the expansion capacity of the channel became stronger, and a large amount of Al melt reacted with the inner Ti fibers along the crushing channel. Moreover, the movement of Al melt under the action of Lorentz force was intensified, and there was a strong collision between Al melt and Al_3Ti layer continuously, the reaction was accelerated.

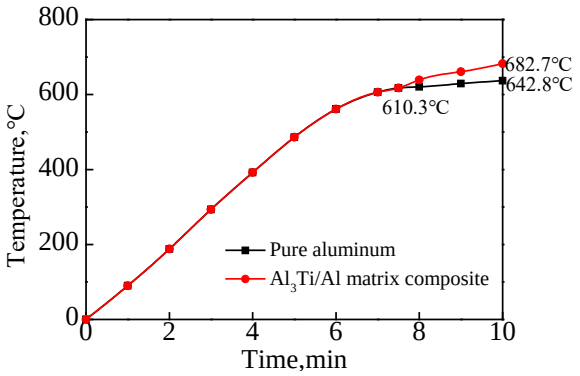

Fig. 6. Real-time temperature curve of pure aluminum and composites at 1 kHz and 10A

Fig. 6 shows the time-temperature curves of pure aluminum and composites under 1 kHz and 10 A. The initiation temperature and initiation time of the Al-Ti reaction were reduced to 610.3 ℃ and 7 min 30 s respectively.

The Ti fiber was completely reacted with the Al melt until the frequency and current increase to 5 kHz and 15 A respectively, and Al_3Ti was dispersed into the Al matrix, as shown in Fig. 7 a. A magnified observation of the Al_3Ti particles in Fig. 7 b revealed that the size of Al_3Ti was refined to 1 – 2 μm and the distance between particles was increased to about 5 μm, which were the optimal values under all parameters.

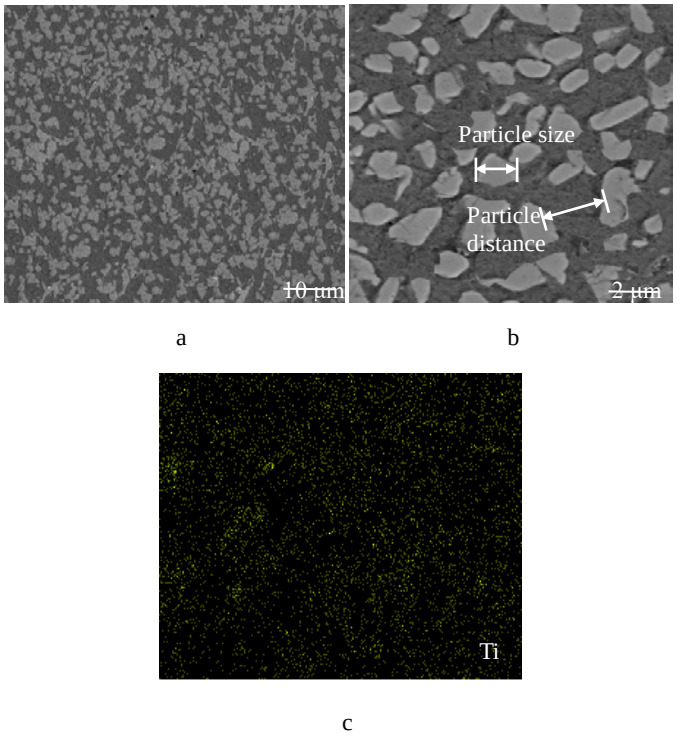

a b

c

Fig. 7. Al_3Ti/Al composites under 5 kHz and 15 A: a – low magnification; b – high magnification; c – surface scanning of Ti

According to the theory of electromagnetic induction, the Lorentz force applied to the particles is increased with the increased frequency and current [12], resulting in the Al_3Ti layer being broken and peeled off easily. Moreover, the mobility of Al_3Ti that has been peeled off to the melt was enhanced due to the increased fluidity of the Al melt, and the area of the matrix covered by Al_3Ti was increased. The Ti element distribution area as shown in Fig. 7 c which indicated that the Ti had been diffused into each area of the Al matrix.

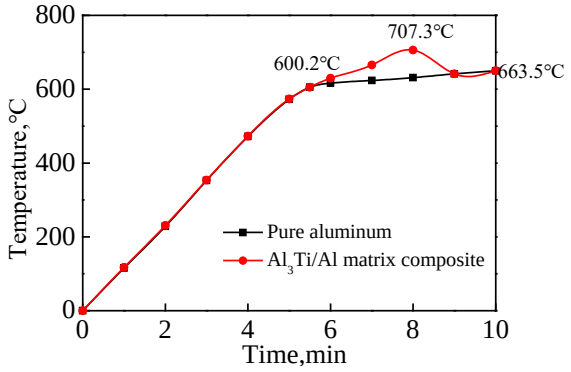

Fig. 8. Real-time temperature curve of pure aluminum and composites at 5 kHz and 15 A

The time-temperature curve of pure aluminum and composites under 5 kHz and 15 A are shown in Fig. 8. The temperature curves were separated at 600.2°C, and the temperature in the composites finally rose to the highest temperature of 707.3°C, proving that the Ti fiber was completely reacted.

When the frequency was fixed at 5 kHz and the current was increased to 20 A, the shape of the product not only had an isometric shape, but also had many long strip shapes, as shown in Fig. 9. The point EDS analysis was carried out on the elongated product to obtain the atomic ratio of elements at different positions as shown in Table 3. The atomic ratio of Al/Ti at points (1)(2)(3) were 3:1, which revealed that the elongated product was Al_3Ti. In addition, previous studies have shown that AlTi and $AlTi_3$ could be formed in theAl-Ti system. However, the formation temperature of AlTi and $AlTi_3$ is 900 ℃ – 1000 ℃ which is higher than the system temperature in this experiment [13]. Therefore, it is further determined that the long product is Al_3Ti.

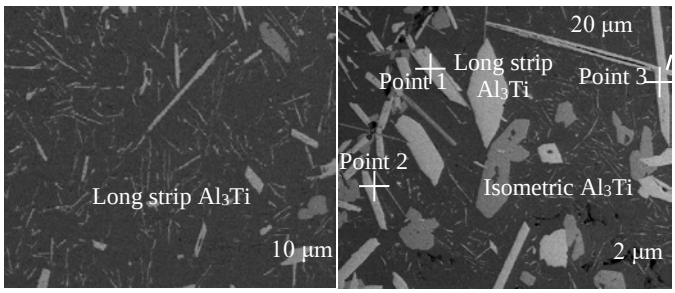

a b

Fig. 9. Al_3Ti/Al composites under 5 kHz and 20 A: a – low magnification; b – high magnification

Table 3. Phase EDS analysis of different point position

No.	Point 1	Point 2	Point 3
Al, at. %	75.18	77.21	76.65
Ti, at.%	24.82	22.79	23.35
Total	100	100	100

The time-temperature curve of the composites under this parameter changes compared with other parameters, as shown in Fig. 10. The temperature reached the maximum value of 716.4 °C when the experience was carried out for 7 minutes, at which Ti was completely reacted. As the experiment continued to 9 minutes, the composites temperature curve that had fallen rose again. In the end, the temperature curve did not overlap, proving that the reaction occurred again in this Al-Ti system. Judging by the point EDS analysis and the time-temperature curve, the formation of elongated shapes of Al_3Ti was the secondary growth of primary Al_3Ti caused by the rose of system temperature.

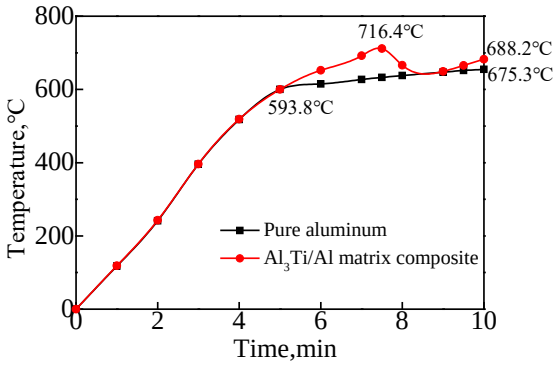

Fig. 10. Real-time temperature curve of pure aluminum and composites at 5 kHz and 20 A

When the current frequency was fixed at 15 A and the frequency was increased to 10 kHz, the Ti fiber was the original shape, showing a regular circle (Fig. 11 a). As the observation magnification was increased, no products were found around the Ti fiber (Fig. 11 b), confirming that no reaction between Al-Ti occurred. In addition, the time-temperature curves of pure aluminum and composites (Fig. 12) were nearly the same during the experiment. At the end of the experience, the temperature was only raised to 395 °C, which was much lower than the Al-Ti reaction temperature.

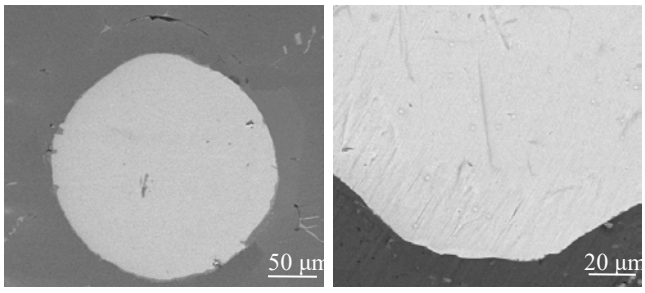

Fig. 11. Al_3Ti/Al composites under 10 kHz and 15 A: a – low magnification; b – Al/Ti edge area

Based on the results of the pre-researches [14], the microstructure of the composites which were prepared in the same preform process and was heated by the best resistance furnace heating parameters (750 °C, 30 min) is shown in Fig. 13. The Ti fiber was completely reacted to form Al_3Ti particles; however, the particles did not move outward (Fig. 13 a). The large area of the Al matrix was not covered by Al_3Ti, as shown in the red area.

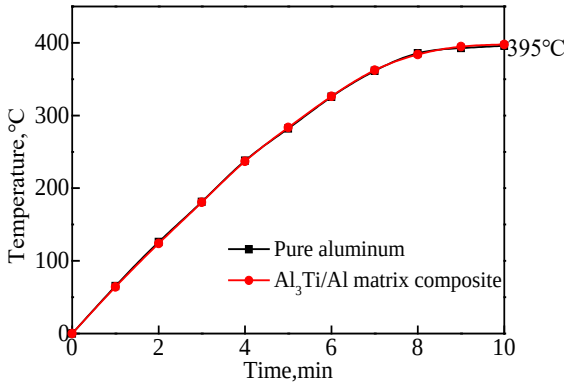

Fig. 12. Real-time temperature curve of pure aluminum and compositels at 10 kHz and 15 A

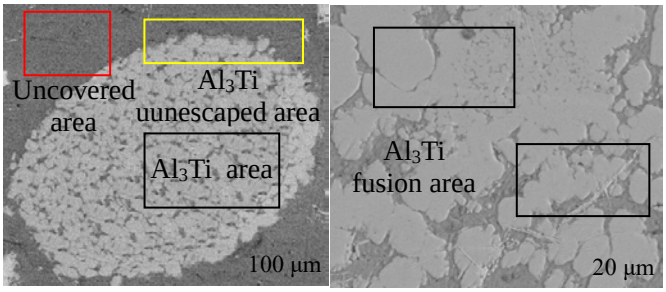

Fig. 13. Microstructure of composites at 750 °C and 30 min: a – low magnification; b – Al_3Ti fusion area

As the Al_3Ti particles area was magnified as shown in Fig. 13 b, it was found that the gaps were so narrow that the particles were merged into one particle gradually, resulting in the size increase to 30 μm – 50 μm. Based on the microstructure of the composites under different heating methods, it was judged that the induction heating has an optimization effect on the dispersion and size of the particles.

3.3. Wear resistance of composites

Fig. 14 shows the wear rate of the composites under different parameter combinations.

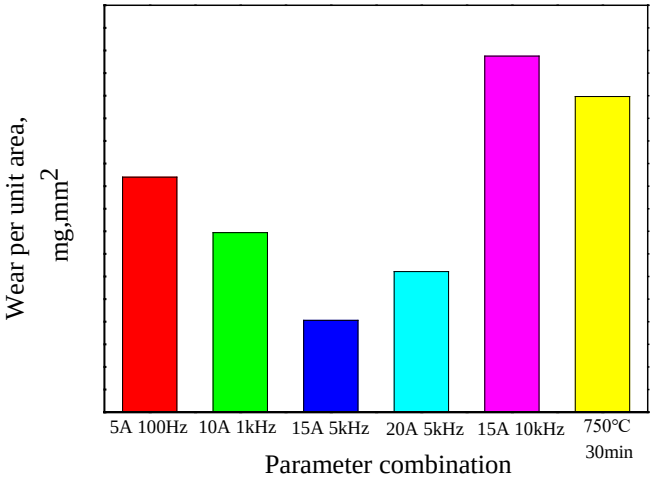

Fig. 14. Effect of different parameter combination on the wear rate of composites

As the frequency and current were increased to 5 kHz and 15 A respectively, the wear rate of the composites was reduced to a minimum value of 2.325 mg/mm^2, which was also lower than that of composites heated by resistance furnace. Whether the current was increased to 20 A or the frequency was increased to 10 kHz, the wear rate was increased. Therefore, the wear resistance of composites could not be improved by increasing frequency and current blindly. To investigate the wear mechanism of each specimen, the SEM images of the wear surfaces were acquired and illustrated in Fig. 15. As the frequency and current were increased to 5 kHz and 15 A respectively, the wear rate of the composites was reduced to a minimum value of 2.325 mg/mm^2, which was also lower than that of composites heated by resistance furnace. Whether the current was increased to 20 A or the frequency was increased to 10 kHz, the wear rate was increased. Therefore, the wear resistance of composites could not be improved by increasing frequency and current blindly.

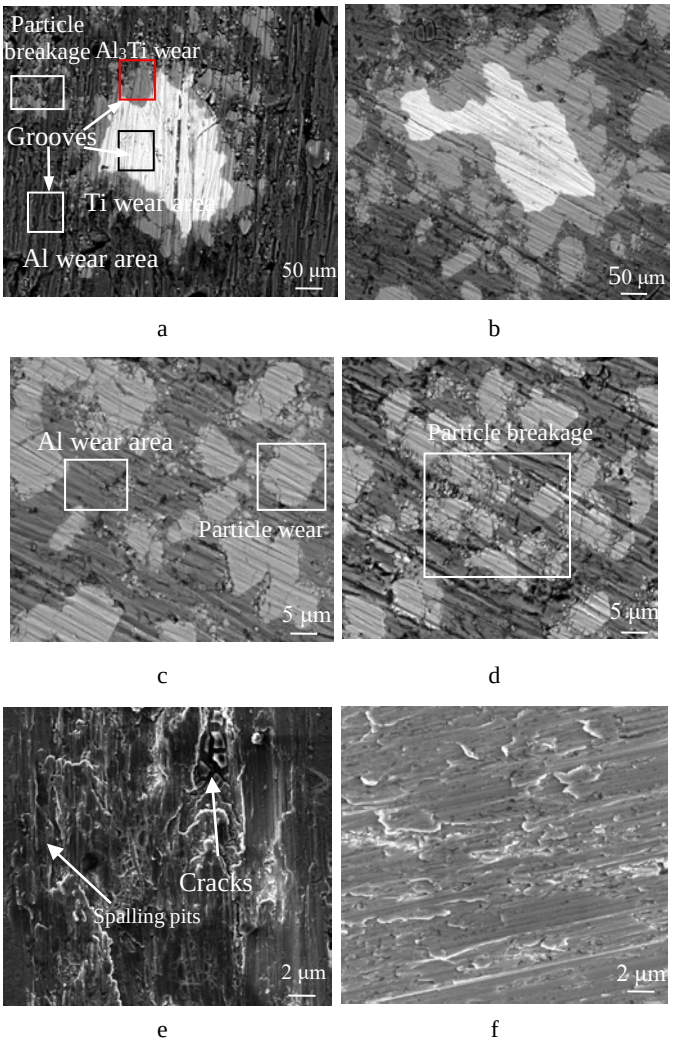

Fig. 15. Wear morphology of composites under different parameter combination: a – 100 Hz 5 A; b – 1 kHz 10 A; c – 5 kHz 15A; d – 5 kHz 20A; e – 10 kHz 15 A; f – 750 °C 30 min

As the frequency and current were increased to 5 kHz and 15 A respectively, the wear rate of the composites was reduced to a minimum value of 2.325 mg/mm^2, which was also lower than that of composites heated by resistance furnace. Whether the current was increased to 20 A or the frequency was increased to 10 kHz, the wear rate was increased. Therefore, the wear resistance of composites could not be improved by increasing frequency and current blindly.

4. RESULTS AND DISCUSSION

4.1. Mechanism of reaction promoted by induction heating

According to the time-temperature curves of the composites, the initiation temperature of the Al-Ti reaction was about 600 °C, which was lower than the reaction temperature of Al-Ti in general heating equipment, and the reaction cycle was shortened. The above test results are related to the magnetic field generated in the induction heating device. The reactant is magnetized to obtain magnetization energy in the magnetic field, leading to the free energy of the reaction atom is increased [15]. Subsequently, the reaction atoms are transitioned to a high-energy and unstable state.

For the exothermic reaction of Al-Ti, to transform into the product finally, it is necessary to give enough energy to form intermediate substances first. Therefore, when Al and Ti atoms are given high energy in the magnetic field, they are transformed into unstable magnetically activated molecules-Al*, Ti* [16] (* means magnetization). The first step of the magnetization reaction is completed:

$$\mathrm{Al} + \mathrm{Ti} + \mathrm{E} \rightarrow \mathrm{Al}^* + \mathrm{Ti}^* . \quad (1)$$

Compared with Al and Ti atoms without the action of a magnetic field, the metal bond between Al* and Ti* atoms after magnetization are polarized and elongated [17], and they are easily broken. When the energy in the magnetic field is large enough to break the metal bond in Al* and Ti*, the Al and Ti are replaced by each other to form a new metal bond to form Al_3Ti, and the final process of the magnetization reaction is completed.

$$\mathrm{Al}^* + \mathrm{Ti}^* \rightarrow \mathrm{Al_3Ti} . \quad (2)$$

In addition, the entropy of the Al-Ti system is affected by the magnetic field at the same time [16]. Due to the paramagnetic properties of Al and Ti, the movement of electrons in them are transformed from disorder to order under the influence of a magnetic field. On the contrary, Al_3Ti is diamagnetic causing the movement of electrons to be transformed more disorderly. It is judged that the difference in entropy between the product and the reactant is increased after applying a magnetic field, that is, the spontaneity of the reaction is increased, and the Al-Ti in-situ reaction is promoted.

4.2. Changing mechanism of microstructure

As the frequency and current were increased from 100 Hz and 5 A to 5 kHz and 15 A respectively, the total heat in the system was increased, the Ti fiber was completely reacted, and the product was granular Al_3Ti. However, when the frequency was increased to 10 kHz, there was no reaction between Al-Ti in the sample. And

when the current was increased to 20 A, the shape of Al_3Ti was transformed into a long strip.

When the frequency was increased to 10 kHz, the core temperature of the composites was 400 ℃, which was lower than the initiation temperature of the Al-Ti reaction significantly. The heat distribution in the sample is concentrated on the surface as the frequency is increased, i.e., the skin effect [18]. The depth of skin effect (δ) can be calculated by

$$\delta = \sqrt{\frac{1}{u\sigma\sigma f}} \ , \tag{3}$$

where ρ is the resistivity of the workpiece; f is the frequency of the power supply; μ is the relative permeability of the workpiece. It is indicated that the depth of skin effect is decreased by increasing the frequency of alternating current. Under the condition of the same sample size, the higher the frequency, the more heat is distributed on the surface of the sample. As a result, the temperature of Ti fiber region is so low that Al-Ti reaction cannot be started due to the thin heated layer.

When the current was increased to 20 A, the shape of Al_3Ti was transformed from equiaxed to elongated. Inferred from the time-temperature curve of the composites at 20 A, when the temperature of the system rises for the second time at 9 minutes, the Ti fiber had been completely reacted before. It was proved that the Ti source required in the secondary growth of Al_3Ti came from the partial melting of primary Al_3Ti. In addition, along with the partial melting of Al_3Ti, the shape of the regenerated Al_3Ti was affected by the unit cell type and the magnetic field.

In the steady-state, the unit cell type of Al_3Ti is $D0_{22}$, which contains nine covalent bonds [19], as shown in Table 4. Based on the principle that the greater the number of covalent electrons in the covalent bond, the stronger the binding ability, so the four metal bonds of A, B, C, and D are arranged in order from large to small according to the binding force, and their respective positions in the crystal structure of Al_3Ti are shown in Fig. 16.

Table 4. Covalent bond structure in Al_3Ti

No.	Covalent bond type	Number of covalent bonds	Number of covalent electrons
A	Al_2-Ti	8	0.3990
B	Al_1-Al_1	8	0.2675
C	Al_1-Ti	16	0.2122
D	Al_1-Al_2	16	0.1422
E	$Ti-Ti$	4	0.0078
F	Al_1-Al_1	8	0.0035
G	Al_2-Al_2	4	0.0035
H	Al_1-Al_1	4	0.0006
I	Al_2-Ti	4	0.0009

During the melting-re-growth process of Al_3Ti, the melting speed of the plane (001) with a strong bonding force of A and B metal bonds is lower than that of the plane (010) with C and D metal bonds, and the growth rate is greater than a plane (010).

Moreover, the generation rate of the strong bonding surface in the crystal structure is promoted by the magnetic field, which causes the growth rate of the plane (001) to increase significantly [20]. Finally, the crystal structure of Al_3Ti is transformed into $D0_{23}$, forming a long strip of Al_3Ti. However, the long strip of Al_3Ti is difficult to be refined, resulting in a vicious influence on the wear resistance of composites.

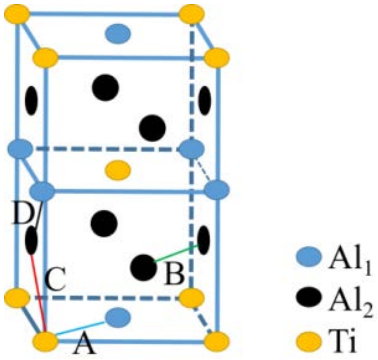

Fig. 16. Covalent bond structure in Al_3Ti

Moreover, [20] the generation rate of the strong bonding surface in the crystal structure is promoted by the magnetic field, which causes the growth rate of the plane (001) to increase significantly. Finally, the crystal structure of Al_3Ti is transformed into $D0_{23}$, forming a long strip of Al_3Ti. However, the long strip of Al_3Ti is difficult to be refined, resulting in a vicious influence on the wear resistance of composites.

4.3. Mechanism of abrasion resistance enhancement

When 100 Hz and 5 A were increased to 5 kHz and 15 A respectively, the wear resistance of the composites was improved. On the one hand, the generation and dispersibility of Al_3Ti are increased, so that the Al matrix and Ti fibers with low hardness are covered by Al_3Ti with high hardness and high wear resistance. On the other hand, the movement in the melt is accelerated and the heat dissipation capacity is enhanced correspondingly, thereby reducing the thermal stress between the Al_3Ti and the Al melt. Finally, Al_3Ti is formed on the Al matrix smoothly, and the bonding force with the matrix is greatly enhanced. It is indicated that the Al matrix is protected by Al_3Ti continuously during the two-body abrasive wear test, and the three-body abrasive wear caused by the flaking of Al_3Ti is reduced.

However, when the current was increased from 15A to 20A, the wear resistance of the composites decreased due to the shape of Al_3Ti mainly. During the wear process of the composites and the abrasive particles, the stress imposed on the long strip of Al_3Ti with sharp edges and corners is much greater than that of the equiaxed Al_3Ti [21], causing the degree of wear and peeling of the Al_3Ti is aggravated. When the frequency was increased to 10 kHz, the Al-Ti reaction was not started due to the skin effect, and no Al_3Ti particles were formed in the sample. During the friction and wear process, a large amount of low-hardness Ti and Al are peeled off, causing the composites to be worn seriously.

5. CONCLUSIONS

In the experiment, Ti fiber (Ø 200 μm, 99.8 wt.%) and pure aluminum (99.6 wt.%) are selected as the reaction

source and matrix, respectively. To ensure the uniformity of the nascent particles, the reaction source is fixed in the matrix at equal intervals. Subsequently, induction heating with different frequencies and current values is applied to promote the Al-Ti reaction. Finally, Al matrix composites reinforced by Al_3Ti with small size and high dispersibility are prepared.

1. As the frequency and current are increased to 5 kHz and 15 A, the Ti fiber is completely reacted to form Al_3Ti. The equiaxed Al_3Ti combined with the matrix smoothly, the size is 1 – 2 μm, and the particle spacing is 5 μm, which are the best microstructure under all parameters. After the current is increased to 20 A, the shape of Al_3Ti is transformed into a long strip under the influence of its crystal structure and the magnetic field. When the frequency is increased to 10 kHz, the Al – Ti reaction does not occur because of the skin effect, no Al_3Ti is formed.
2. The wear rate of the composites at 5 kHz and 15 A is 2.325 mg/mm^2, reaching the optimal values in this experiment. Under this parameter, the width and depth of the grooves on Al_3Ti and Al become narrower and shallower respectively, and the Al_3Ti particles are intact.

Acknowledgments

Open topic of Shaanxi Key Laboratory of Nano-materials and Technology, Xi'an University of Architecture and Technology (18JS060) and (18JS075); Science and Technology Project of China Huaneng Group (HNKI18-H45).

REFERENCES

1. **Barenji, R.V., Khojastehnezhad, V.M., Pourasl, H.H., Rabiezadeh, A.** Wear Properties of Al-Al_2O_3/TiB_2 Surface Hybrid Composite Layer Prepared by Friction Stir Process *Journal of Composite Materials* 50 (11) 2015: pp. 1457 – 1466. https://doi.org/10.1177/0021998315592007
2. **Habibolahzadeh, A., Hassani, A., Bagherpour, E.** Dry Friction and Wear Behavior of In-situ Al/Al_3Ti Composite *Journal of Composite Materials* 48 (9) 2014: pp. 1049 – 1059. https://doi.org/10.1177/0021998313482153
3. **Zeng, Y., Himmler, D., Randelzhofer, P.** In Situ Al_3Ti/Al Composites Fabricated by High Shear Technology: Microstructure and Mechanical Properties *Materials Science and Technology* 35 (18) 2019: pp. 1 – 10. https://doi.org/10.1080/02670836.2019.1677025
4. **Liu, Z.W., Cheng, N., Zheng, Q.L., Wu, J.H.** Processing and Tensile Properties of A356 Composites Containing in Situ Small-Sized Al_3Ti Particulates *Materials Science and Engineering A* 710 2018: pp. 392 – 399. https://doi.org/10.1016/j.msea.2017.11.005
5. **Qin, J., Chen, G., Wang, B.** Formation of In-Situ Al_3Ti Particles from Globular Ti Powders and Al Alloy Melt under Ultrasonic Vibration *Journal of Alloys & Compounds* 653 2015: pp. 32 – 38. https://doi.org/10.1016/j.jallcom.2015.09.005
6. **Gupta, R., Daniel, B.S.S.** Impression Creep Behaviour of Ultrasonically Processed In-situ Al_3Ti Reinforced Aluminium Composite *Materials Science and Engineering A* 733 2018: pp. 257 – 266. https://doi.org/10.1016/j.msea.2018.07.017
7. **Liu, Z., Rakita, M., Wang, X., Han, Q.** In Situ Formed Al_3Ti Particles in Al Alloy Matrix and Their Effects on The Microstructure and Mechanical Properties of 7075 Alloy *Journal of Materials Research* 29 (12) 2014: pp. 1354 – 1361. https://doi.org/:10.1557/jmr.2014.123
8. **Yan, Y.T., Niu, L.B., An, Y.J.** Effect of Frequency on Microstructure and Properties of In-situ Synthesized Al_3Ti/Al Composites *Rare Metal Materials and Engineering* 49 (06) 2020: pp. 2175 – 2181. https://doi.org/1002-185X(2020)06-2175-07
9. **Ye, Y., Li, P., He, L.** Valence Electron Structure Analysis of Morphologies of Al_3Ti and Al_3Sc in Aluminum Alloys *Intermetallics* 18 (2) 2010: pp. 292 – 297. https://doi.org/10.1016/j.intermet.2009.07.023
10. **Ghosh, G., Walle, A.V.D., Asta, M.** First-Principles Phase Stability Calculations of Pseudobinary Alloys of $(Al,Zn)_3Ti$ with $L1_2$, $D0_{22}$, and $D0_{23}$ Structures *Journal of Phase Equilibria and Diffusion* 28 (1) 2007: pp. 9 – 22. https://doi.org/10.1007/s11669-006-9007-4
11. **Ma, J., Niu, L.B., Wu, H., Gao, C., An, Y.J.** Formation and Wear Behaviors of In-Situ Al_3Ti/Al Composites Using Aluminum and Titanium Fibers Under Electromagnetic Induction Heating *Journal of Central South University* (27) 2020: pp. 3594 – 3602. https://doi.org/10.1007/s11771-020-4500-1
12. **Zhang, W., Zhao, G., Fu, Q.** Study on the Effects and Mechanisms of Induction Heat Treatment Cycles on Toughness of High Frequency Welded Pipe Welds *Materials Science and Engineering A* 736 (24) 2018: pp. 276 – 287. https://doi.org/10.1016/j.msea.2018.09.004
13. **Rzyman, K., Moser, Z., Gachon, J.C.** Calorimetric Studies of the Enthalpies of Formation of Al, Ti, AlTi, $AlTi_3$ and Al_2Ti Compounds *Archives of Metallurgy and Materials* 49 (3) 2004: pp. 545 – 563. https://doi.org/10.1128/IAI.68.11.6423-6430.2000
14. **Yu, J., Niu, L.B., Cai, A.J.** Influence of Holding Temperature on Microstructure of Product Al_3Ti in Al Matrix Composite *Hot Working Technology* 46 (20) 2017: pp. 134 – 136. https://doi.org/10.14158/j.cnki.1001-3814.2017.20.035
15. **Agrawal, S., Ghose, A.K., Chakrabarty, I.** Effect of Rotary Electromagnetic Stirring During Solidification of In-Situ Al-TiB_2 Composites *Materials & Design* 113 2017: pp. 195 – 206. https://doi.org/10.1016/j.matdes.2016.10.007
16. **Li, G.R.** Microstructure Control and Properties of In Situ Fabricating Particulate Reinforced Aluminum Matrix Composites. PhD Thesis, Jiang Su University, 2007.
17. **Li, G.R., Wang, H.M., Zhao, Y.T.** Microstructure of in Situ Al_3Ti/6351Al Composites Fabricated with Electromagnetic Stirring and Fluxes *Transactions of Nonferrous Metals Society of China* (4) 2010: pp. 45 – 51. https://doi.org/ 10.1016/S1003-6326(09)60181-3
18. **Zhu, X.R., Harding, R.A., Campbel, J.** Electromagnetic Confinement Including the Dynamic Effect Due to Melt Flow *ISIJ International* 39 (1) 2007: pp. 1 – 9. https://doi.org/ 10.2355/isijinternational.39.1
19. **Qin, J.** Study on Ultrasonic-Assisted In-Situ Reaction Preparation and Properties of $TiAl_3$/2024Al Composites. PhD Thesis, Harbin Institute of Technology, 2009.

20. **Liu, W., Li, J.Q., Ding, X.** Development of Microstructure of Semi-Solid A356 Alloy by Alternating Electromagnetic Stirring *Advanced Materials Research* 266 2011: pp. 84 – 88. https://doi.org/10.4028/www.scientific.net/AMR.266.84

21. **Madhu, H.C., Edachery, V., Lijesh, K.P.** Fabrication of Wear-Resistant Ti_3AlC_2/Al_3Ti Hybrid Aluminum Composites by Friction Stir Processing *Metallurgical and Materials Transactions A* 51 2020: pp. 4086 – 4099. https://doi.org/10.1007/s11661-020-05821-1